RSC Advances

ROYAL SOCIETY OF CHEMISTRY

www.rsc.org/advances

Journal Name

RSCPublishing

ARTICLE

Gradual thickness-dependent enhancement of the thermoelectric properties of PEDOT: PSS nanofilms

Cite this: DOI: 10.1039/x0xx00000x

Received 00th January 2012,
Accepted 00th January 2012

DOI: 10.1039/x0xx00000x

www.rsc.org/

Dohyuk Yoo,[a] Woohyun Son,[a] Seyul Kim,[a] Jung Joon Lee,[a] Seung Hwan Lee,[a] Hyang Hee Choi,[b*] and Jung-Hyun Kim,[a*]

We have investigated the thickness-dependent change in the thermoelectric properties of nanofilms of the conducting polymer, PEDOT:PSS. Films with varying thickness were prepared by spin coating the polymer solution at different speeds. Because of its relatively facile processing, good electrical conductivity, and environmental stability, PEDOT:PSS is considered to be one of the most promising candidates for application in thermal to electric energy conversion devices. Electrical conductivity is attributed to the enhanced carrier mobility in the ordered chain structures of the polymer. The Seebeck coefficient is influenced by the energy derivative of electronic energy density. This approach can be used to study the dependence of conductivity and the Seebeck coefficient at room temperature with varying film thickness. Both the conductivity and Seebeck coefficient improved with increasing thickness of the polymer nanofilms. This can be attributed to the change in the conformation of PEDOT, which exposes the PEDOT on the surface of the PEDOT:PSS phase. The PEDOT:PSS thin films were characterized by UV-Vis spectroscopy, tapping-mode atomic force microscopy, X-ray photoelectron spectroscopy, and Raman spectroscopy. This study suggests that variation of film thickness is an effective way of improving the thermoelectric properties of PEDOT:PSS.

Introduction

The global energy crisis and alarming environmental problems have greatly motivated research on the technological development of new energy resources. In this context, thermoelectric (TE) materials have attracted significant interest in recent years due to their potential for generating power from waste heat.[1-4] The performance of TE materials is determined by a dimensionless quantity, the figure of merit (ZT), given by the following equation:

$$ZT = (\sigma S^2)/\kappa T \quad (1)$$

where, σ, S, κ and T represent the electrical conductivity, Seebeck coefficient, thermal conductivity, and absolute temperature, respectively. The expression σS^2, known as the power factor, is generally used to evaluate the TE performance of similar materials. To obtain an excellent ZT performance at room temperature, a high power factor and a low κ value are required. It is proposed that the best TE material should possess thermal properties similar to that of glass and electrical properties similar to that of a perfect single crystal material like phonon glass electron crystal (PGEC).[5-7]

Till date, the most widely researched TE materials include semiconductors and metal alloys, such as Bi_2Te_3,[8,9] PbTe,[10-12] SiGe,[13,14] filled $CoSb_3$ skutterudites, and clathrates.[8,15-17] Despite the high power factor of these inorganic TE materials, their drawbacks such as high cost of raw materials, poor processability, potential for heavy metal pollution, and high thermal conductivity restrain their wider practical applicability. An alternative approach to the research on TE materials, which involves the use of conducting polymers, has remained a relatively unexplored domain. Conducting-polymer-based TE materials are very attractive options owing to their intrinsic low

thermal conductivity and high electrical conductivity. Typically, the thermal conductivity of a conducting polymer ranges from 0.08 to 0.6 W/mK, which is two orders of magnitude below that of inorganic TE materials.[18,19] In addition to this, the low cost of fabrication, ease of processing, environmental stability, and less-toxicity of conducting polymers render them more suitable for utilization as TE materials.

In recent times, increasing efforts have been devoted to the development of TE materials based on conducting polymers. These chiefly include polyacetylene, polyaniline (PANI), polythiophene (PTs), polypyrrole (PPy), and their derivatives.[20-25] Among these conducting polymers, poly (3, 4-ethylenedioxythiophene) (PEDOT) has drawn particular attention.[26] PEDOT is a derivative of polythiophene and possesses high electrical conductivity, excellent transparency, and environmental stability. It can be processed in an aqueous solution with poly (4-styrene sulfonic acid) (PSS) in the appropriate ratio to form a hole-conducting polymer blend PEDOT:PSS (chemical structure shown in Fig. 1). PEDOT:PSS is widely used as an antistatic coating material, field-effect transistor, and as an electrode material for devices like capacitors, photodiodes, and solar cells. In the context of its thermoelectric properties, a large amount of research has been carried out to improve the electrical conductivity and Seebeck coefficient of PEDOT: PSS.[27,28] Polar organic compounds with high boiling point, e.g., dimethyl sulfoxide (DMSO),[29-31] ionic liquids,[32,33] and carbon nanotubes/ graphene[34,35] have been investigated as additives for progressive effects on the electrical conductivity of PEDOT:PSS. The Seebeck coefficient of PEDOT:PSS has also been tuned by doping with ammonium formate and urea and by forming a PEDOT:PSS/Bi_2Te_3 composite.[36,37]

In addition to doped PEDOT:PSS systems and PEDOT:PSS-based composites, nanofilms of PEDOT:PSS have generated significant research interest. Generally, spin coating is the preferred method for fabrication of PEDOT:PSS-based nanofilms. Spinning speed (described in rpm) is one of the most important parameters of the spin coating process, responsible for the final quality of the TE nanofilm. The spinning speed affects the thickness, surface quality, and even the composition of the final nanofilm. However, this factor has not been studied or effectively explored till date. In this light, a detailed and systematic study focusing on the effect of spinning conditions (in the spin coating process) on the nature and properties of the fabricated polymer nanofilms is indeed critical. In this study, we have fabricated PEDOT:PSS-based TE nanofilms using a spin coating approach and systematically investigated the effects of the spinning speed on the surface states, composition, and performance of these TE films.

Experimental

Preparation of PEDOT:PSS nanofilms

Bare glass substrates were treated with oxygen (O_2) plasma for 5 min to enhance the hydrophilicity of the surface. The PEDOT:PSS was purchased from Polymertiz Co. Ltd (TCF-A40). Commercial PEDOT:PSS aqueous solution was filtered using a syringe filter (Nylon membrane with 1 μm pore size, Membrane Solutions) prior to use. PEDOT:PSS films with varying thickness were prepared by spin coating the PEDOT:PSS solution onto the glass substrates at various spin rates ranging from 300 rpm to 1500 rpm. The films were subsequently annealed for 10 min at 150 Celsius degrees (℃) on a hot plate.

Coating characterization

The UV-Vis absorption of the PEDOT:PSS films on glass substrates was measured by a wide range spectrophotometer (Lambda 750, PerkinElmer). Photoemission experiments were performed using an X-ray photoelectron spectrometer (XPS, K-alpha, Thermo UK.) equipped with a monochromatic AI Kα X-ray source (1486.6 eV). Raman spectra of the films were obtained by a Raman spectrometer (LabRam Aramis, Horriba Jovin Yvon) using a Nd:Yag laser source with a wavelength of 532 nm. The surface morphology was investigated by atomic force microscopy (AFM, Dimension 3100, Digital Instrument Co.). The electrical conductivities of the PEDOT:PSS films were calculated from the sheet resistance and thickness measured by using the Van der Pauw method with a four-point contact configuration by a Keithley 2400 source-measure unit, 2182 nanovoltmeter, 7001 switch system, and a surface profiler (alpha step IQ, KLA-Tencor).

Film measurement

Two Peltier devices were attached to an aluminium heat sink using a thermal compound to avoid thermal disturbances and maintain a controlled temperature gradient. Current was controlled using a Keithley 2400 source meter resulting in a temperature gradient of 5℃. To measure the temperature gradient across the films, two T- type thermocouples were used. Silver paste was deposited onto the surface of each PEDOT:PSS film with space intervals of 10mm for electrical contact and dried in a vacuum oven at 100℃ for 1 h. The thermal conductivity (k) of PEDOT:PSS was measured using a laser flash apparatus (Netzsch LFA 457 MicroFlash Instruments Inc.) with a xenon flash lamp; k is related to the thermal diffusivity, specific heat, and density, according to the relationship $k=DC_pd$. Precise values of the specific heat were determined using a differential scanning calorimeter (DSC Q20, TA instruments, New Castle, DE) in vacuum. The carrier mobility and carrier concentration of PEDOT:PSS nanofilms were measured by using hall effect measurement system (HMS-3000, ECOPIA Co.).

Results and discussion

PEDOT:PSS is generally synthesized by an oxidative polymerization process catalyzed by metal cations, the universal oxidant present in various organic solvent systems. In

the dissolved PSS medium, the oxidant oxidizes EDOT monomers to form a cationic radical structure. This unstable radical proceeds to form a stable dimer by reaction steps that involve combination and deprotonation. Continuous recurrence of these steps results in the formation of well-dispersed and in-situ doped PEDOT:PSS solution. Fig. 1 shows the chemical structures of 3, 4-ethylenedioxythiophene (EDOT) and poly (3, 4-ethylenedioxythiophene) (PEDOT). The structure of the as-prepared PEDOT is made up of the benzoid and quinoid forms.

Table 1. Thermal properties of PEDOT : PSS thickness at room temperature.

Spin rate (r.p.m.)	Thickness (nm)	Seebeck coefficient (uV K^{-1})	Conductivity (S cm^{-1})	Power factor (uW mK^{-2})	Thermal conductivity (W $m^{-1}K^{-1}$)	ZT ($\times 10^{-3}$)
300	357	24.1	18.1	1.05	0.23[a]	1.37
500	199	23.1	17.5	0.93		1.21
1000	116	21.0	16.6	0.73		0.95
1500	89	17.5	15.9	0.49		0.64

[a] This value was obtained in the bulk pellet.

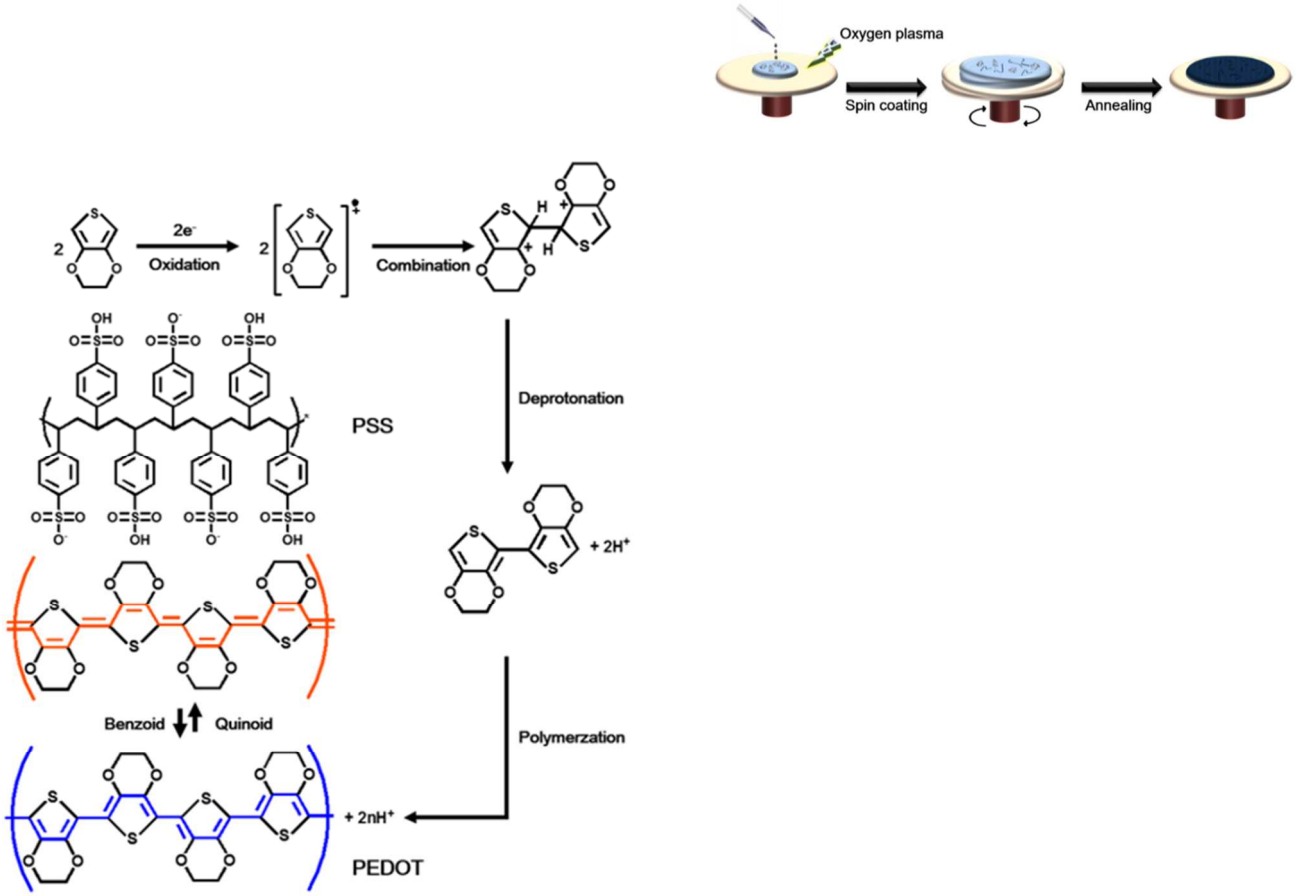

Figure 1. Chemical structure of conjugated conductive polymer poly(3,4-ethylenedioxythiophene) (PEDOT) : Poly(4-styrene sulfonic acid) PSS.

The benzoid structure possesses a π-electron localized, conjugated structure that remains largely unaffected by external causes. In contrast, the quinoid form of PEDOT possesses a delocalized state of π-electrons, which can be affected by solvent treatment.[38] In the electrically active, oxidized state, there is a positive charge on every monomer unit of the PEDOT polymer chain. This charge on the backbone is balanced with an anion that may be either a small molecule or a macromolecular anion such as poly (4-styrene sulfonic acid) (PSS).

The nanofilms were prepared by spin coating the PEDOT:PSS solution onto the glass substrates at various spin rates ranging from 300 rpm to 1500 rpm. Fig. 2 shows a schematic view of the solution coating processes for oxygen plasma treatment, micropipette dropping, and spin coating. These nanofilms were kept in an oven at 150℃ for 10 min to remove the solvent. The thickness of the PEDOT:PSS nanofilms has an

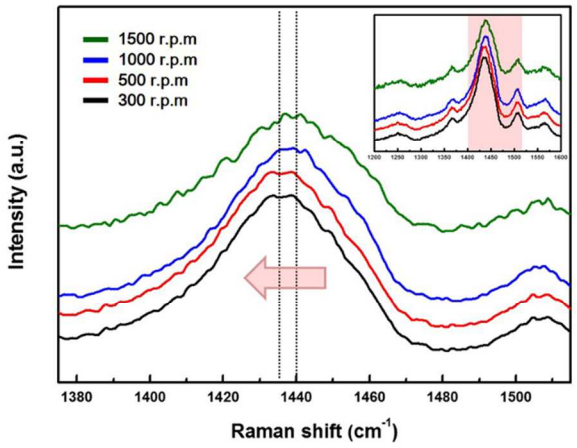

important effect on the device performance because the conductivity changes with the film thickness (Table 1 and Fig. S1).

Figure 2. Schematic diagrams of the solution coating processes for spin coating.

It is observed that an increase in the thickness results in an improved electrical conductivity. Interestingly, as the film thickness decreases at 89 nm, the conductivity gradually decreases as well. The carrier concentration and mobility of PEDOT:PSS nanofilms were measured by using hall effect measurement system. As film the thickness was decreased from 357 to 89nm, carrier mobility was also decreased from 4.66 to 1.45 cm^2/Vs (Fig. S2). This results were indicated that electrical properties of PEDOT:PSS such as carrier mobility were increased due to occur the phase separation and conformation transition.

The surface morphology of the PEDOT:PSS films has been studied by AFM (Fig. 3a-d). The observed rms roughnesses are 2.097nm (Fig. 3a), 1.312nm (Fig. 3b), 0.839 nm (Fig. 3c), and 0.726nm (Fig. 3d) at varied spin rates from 300 rpm to 1500 rpm.

Figure 3. AFM images of PEDOT : PSS nanofilm thickness. All images captured an area of 2 × 2 μm^2 and scale bar is 1 μm.

Figure 4. Raman spectroscopy of poly (3,4-ethylenedioxythiophene) (PEDOT) : Poly (4-styrene sulfonic acid) materials.

These results are shown phase images of a 2 × 2 μm^2. We presume that the phenomenon of diminished phase separation between PEDOT and PSS occurs due to the decrease in the thickness of coated PEDOT:PSS films.

Raman spectra in Fig. 4 shows the main types of ring stretching vibrations of PEDOT and PSS: namely C-C inter-ring stretching (1260 cm^{-1}); C=C symmetrical stretching(1436 cm^{-1}); C=C asymmetrical stretching (1509 cm^{-1}); and C=C antisymmetric stretching (1567 cm^{-1}).[38,39] The coil and linear or expanded-coil conformations exist in PEDOT:PSS nanofilms. The peak intensities of PEDOT:PSS films spin coated at speeds of 300 rpm and 500 rpm increase at 1260 cm^{-1} and disappear for the spin speeds of 1000 rpm and 1500 rpm. The reason for this phenomenon is the conversion of the PEDOT:PSS coil conformation into the linear or expanded-coil conformation following the enhancement of electrical properties with conductivity and carrier mobility. With a further increase in the film thickness of PEDOT:PSS, there was a slight shift in the C=C symmetrical stretching vibration from 1440 cm^{-1} to 1435 cm^{-1}. This is because thicker nanofilms of low-spin-speed-coated

Figure 5. XPS spectra of sulfur 2p for PEDOT:PSS nanofilms prepared various a) 300 r.p.m, b) 500 r.p.m, c) 1000 r.p.m, and d) 1500 r.p.m thickness.

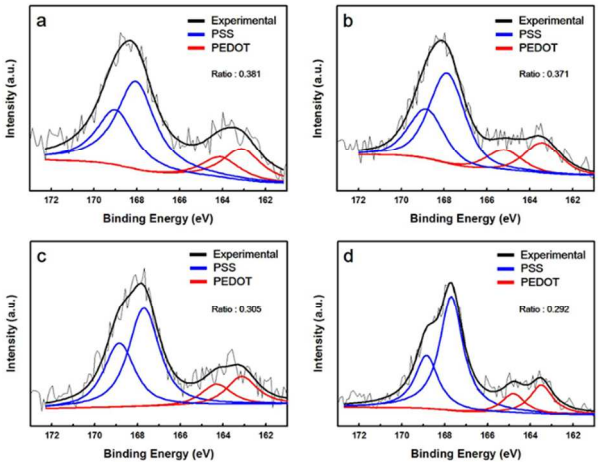

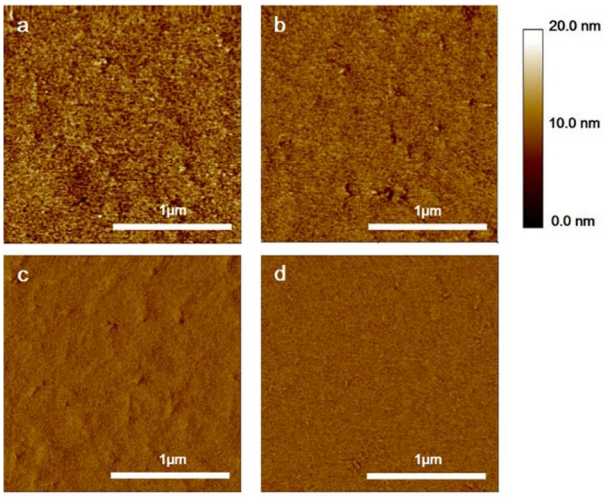

r.p.m.	(a) 300	(b) 500	(c) 1000	(d) 1500
rms (nm)	2.097	1.312	0.839	0.726

Figure 6. The absorbance spectrum of 89 nm ~ 357 nm sized PEDOT : PSS nanofilm measured by UV-Vis spectrophotometer.

PEDOT: PSS preferred the quinoid structure of PEDOT in contrast to the thinner nanofilms.[40]

Fig. 5 shows the XPS spectra of the PEDOT:PSS nanofilms of varying thickness. The XPS band at lower binding energies between 163eV and 166eV correspond to the sulfur atoms in PEDOT. The higher binding energy peak near 169 eV corresponds to the sulfur atom in the PSS dispersant. In the XPS spectra of sulfur, the intensity ratio of S 2p varies with film thickness. The reduction in the surface composition of PEDOT is confirmed by the decreasing PEDOT:PSS intensity ratio in the XPS spectra: 0.381 (Fig. 5a), 0.371 (Fig. 5b), 0.305 (Fig. 5c), and 0.292 (Fig. 5d). This occurs owing to deterioration of the vigorous phase separation in the thinner nanofilms.

The UV-Vis absorbance spectrum of 89 nm ~ 357 nm sized PEDOT:PSS films is shown in Fig. 6. This figure shows the absorbance peaks of PSS dispersant between 200 nm and 360 nm.[41] It is observed that as the thickness of the PEDOT: PSS nanofilms decreases, the UV absorbance intensity of PSS increases due to the overexposure of PSS as compared to the PEDOT grains on the nanofilm surface.

The thermoelectric Seebeck coefficient (S) and its temperature dependence for PEDOT:PSS were determined by using a 0.7 mm copper wire. The hot junction was placed in the thermostage with a reference copper-constantan thermocouple, and the cold

Figure 7. Schematic of seebeck measurement device by two T-type thermocouples.

Figure 8. Thermoelectric properties of PEDOT : PSS nanofilms.

junction between the PEDOT:PSS and copper was thermally anchored at room temperature (25°C). The same anchoring was used for the cold junction of the copper-constantan thermocouple (a diagram of the experimental set-up is shown in Fig. 7). The nature of the electro-motive force measured for PEDOT:PSS thermocouple is presented as a function of temperature difference between the actual hot junction temperature and the room temperature. We thus suggest that the ZT value for the PEDOT:PSS films change with the thickness of the film. The thermoelectric properties, namely, the electrical conductivity, Seebeck coefficient, and the ZT are measured in terms of the thickness differences of the PEDOT:PSS films; these results are Fig. 8. Thermoelectric properties of PEDOT : PSS nanofilms as shown in Fig. 8 and listed in Table. 1. Thermal conductivity for calculating of ZT was measured in the

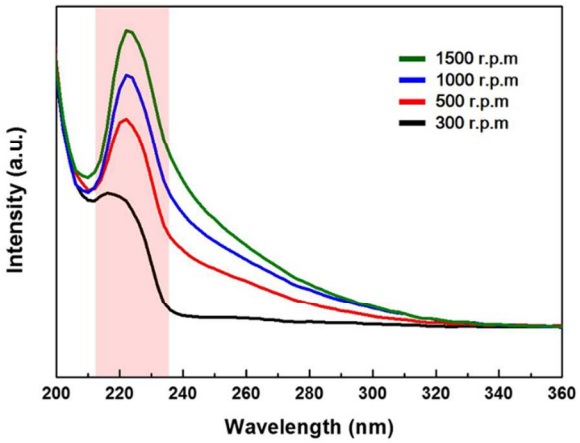

forming of bulk pellet and obtained a value of 0.23 W/mK. The thicker nanofilm (300 rpm coated PEDOT:PSS) exhibited the best properties in terms of the electrical conductivity and Seebeck coefficient, corresponding to an 114% enhancement in ZT values in comparison to the thinnest nanofilm.

Conclusions

We have systematically investigated the dependence of the thickness, surface roughness, composition, and TE performance of PEDOT:PSS nanofilms on spinning speed. It is revealed that the TE properties of PEDOT:PSS films are greatly affected by the conditions of the spinning process. Varying the spinning speed not only changes the thickness of the PEDOT:PSS film, but also affects the composition of the final product, resulting in a change up to three orders of magnitude in the ZT value. Both the Seebeck coefficient and electrical conductivity of the PEDOT:PSS film decrease with an increase in the spinning speed. Using the thermal conductivity of 0.23 W/mK, a PEDOT:PSS film prepared at a spinning speed of 300 rpm shows a maximum ZT of 1.37×10^{-3}. Many researches have shown that the TE properties of PEDOT:PSS can be tuned and improved by either doping or hybridizing methods. This work is aimed at demonstrating the key role of the spinning process in the TE performance of PEDOT:PSS nanofilms. It is expected that our work may help the design and fabrication of PEDOT:PSS-based TE nanofilms in the future.

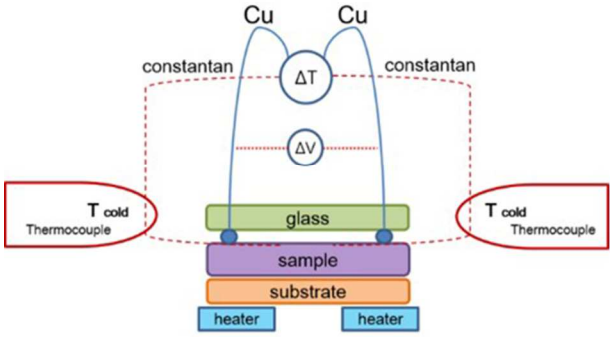

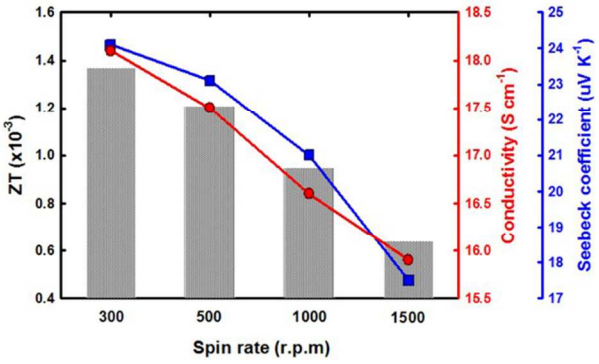

Acknowledgments

This research was supported by the Basic Science Research Program through the National Research Foundation of Korea (NRF) funded by the Ministry of Education, Science and Technology (no. 2012R1A1A3013893). This project was supported by Priority Research Centers Program through the National Research Foundation of Korea (NRF) funded by the Ministry of Education, Science and Technology (2009-0093823). This research was supported by the Pioneer Research Center Program through the National Research Foundation of Korea (NRF) funded by the Ministry of Science, ICT & Future Plannig (2010-0019550).

Notes

[a] Department of Chemical and Biomolecular Engineering, Yonsei University, Seoul 120–749, Republic of Korea
[b] Institute of Nanoscience and Nanotechnology, Yonsei University, Seoul 120–749, Republic of Korea.
† Corresponding authors. Hyang Hee Choi e-mail: netchoi@yonsei.ac.kr; Tel: +82 2 2123 7632; Fax: +82 2 312 0305, Jung-Hyun Kim e-mail: jayhkim@yonsei.ac.kr; Tel: +82 2 2123 7633; Fax: +82 2 312 0305

References

1. J. P. Heremans, M. S. Dresselhaus, L. E. Bell and D. T. Morelli, *Nature nanotechnology*, 2013, **8**, 471.
2. Y. Lan, A. J. Minnich, G. Chen and Z. Ren, *Advanced Functional Materials*, 2010, **20**, 357.
3. J. R. Sootsman, D. Y. Chung and M. G. Kanatzidis, *Angewandte Chemie International Edition*, 2009, **48**, 8616.
4. M. Zebarjadi, K. Esfarjani, M. Dresselhaus, Z. Ren and G. Chen, *Energy & Environmental Science*, 2012, **5**, 5147.
5. T. Kajikawa and D. Rowe, DM Rowe, CRC/Taylor & Francis, Boca Raton, FL, USA, 2006.
6. G. S. Nolas, J. Poon and M. Kanatzidis, *MRS bulletin*, 2006, **31**, 199.
7. A. Minnich, M. Dresselhaus, Z. Ren and G. Chen, *Energy & Environmental Science*, 2009, **2**, 466.
8. R. Venkatasubramanian, E. Siivola, T. Colpitts and B. O'quinn, *Nature*, 2001, **413**, 597.
9. B. Poudel, Q. Hao, Y. Ma, Y. Lan, A. Minnich, B. Yu, X. Yan, D. Wang, A. Muto and D. Vashaee, *Science*, 2008, **320**, 634.
10. J. Androulakis, C.-H. Lin, H.-J. Kong, C. Uher, C.-I. Wu, T. Hogan, B. A. Cook, T. Caillat, K. M. Paraskevopoulos and M. G. Kanatzidis, *Journal of the American Chemical Society*, 2007, **129**, 9780.
11. J. P. Heremans, V. Jovovic, E. S. Toberer, A. Saramat, K. Kurosaki, A. Charoenphakdee, S. Yamanaka and G. J. Snyder, *Science*, 2008, **321**, 554.
12. G. J. Snyder and E. S. Toberer, *Nature materials*, 2008, **7**, 105.
13. X. Wang, H. Lee, Y. Lan, G. Zhu, G. Joshi, D. Wang, J. Yang, A. Muto, M. Tang and J. Klatsky, *Applied Physics Letters*, 2008, **93**, 193121.
14. G. Joshi, H. Lee, Y. Lan, X. Wang, G. Zhu, D. Wang, R. W. Gould, D. C. Cuff, M. Y. Tang and M. S. Dresselhaus, *Nano letters*, 2008, **8**, 4670.
15. B. Sales, D. Mandrus and R. K. Williams, *Science*, 1996, **272**, 1325.
16. G. Nolas, J. Cohn, G. Slack and S. Schujman, *Applied Physics Letters*, 1998, **73**, 178.
17. V. Ponnambalam, P. N. Alboni, J. Edwards, T. M. Tritt, S. R. Culp and S. J. Poon, *Journal of Applied Physics*, 2008, **103**, 063716.
18. J. Yang, H. L. Yip and A. K. Y. Jen, *Advanced Energy Materials*, 2013, **3**, 549.
19. D. Wang, W. Shi, J. Chen, J. Xi and Z. Shuai, *Physical Chemistry Chemical Physics*, 2012, **14**, 16505.
20. Q. Wang, Q. Yao, J. Chang and L. Chen, *Journal of Materials Chemistry*, 2012, **22**, 17612.
21. Q. Yao, L. Chen, W. Zhang, S. Liufu and X. Chen, *Acs Nano*, 2010, **4**, 2445.
22. Y. Zhao, G.-S. Tang, Z.-Z. Yu and J.-S. Qi, *Carbon*, 2012, **50**, 3064.
23. J. Xiang and L. T. Drzal, *Polymer*, 2012, **53**, 4202.
24. Y. Xiao, J.-Y. Lin, S.-Y. Tai, S.-W. Chou, G. Yue and J. Wu, *Journal of Materials Chemistry*, 2012, **22**, 19919.
25. C. Bounioux, P. Díaz-Chao, M. Campoy-Quiles, M. S. Martín-González, A. R. Goñi, R. Yerushalmi-Rozen and C. Müller, *Energy & Environmental Science*, 2013, **6**, 918.
26. R. Dietrich, *Journal of Materials Chemistry A*, 2013, **1**, 7576.
27. H. Park, S. H. Lee, F. S. Kim, H. H. Choi, I. W. Cheong and J. H. Kim, *Journal of Materials Chemistry A*, 2014, **2**, 6532.
28. S. H. Lee, H. Park, W. Son, H. H. Choi and J. H. Kim, *Journal of Materials Chemistry A*, 2014, **2**, 13380.
29. C. Liu, F. Jiang, M. Huang, R. Yue, B. Lu, J. Xu and G. Liu, *Journal of electronic materials*, 2011, **40**, 648.
30. T.-C. Tsai, H.-C. Chang, C.-H. Chen and W.-T. Whang, *Organic Electronics*, 2011, **12**, 2159.
31. M. Scholdt, H. Do, J. Lang, A. Gall, A. Colsmann, U. Lemmer, J. D. Koenig, M. Winkler and H. Boettner, *Journal of electronic materials*, 2010, **39**, 1589.
32. C. Liu, J. Xu, B. Lu, R. Yue and F. Kong, *Journal of electronic materials*, 2012, **41**, 639.
33. A. M. Nardes, R. A. Janssen and M. Kemerink, *Advanced Functional Materials*, 2008, **18**, 865.
34. G. H. Kim, D. H. Hwang and S. I. Woo, *Physical Chemistry Chemical Physics*, 2012, **14**, 3530.
35. D. Yoo, J. Kim and J. H. Kim, *Nano Research*, 2014, **7**, 717.
36. F. Kong, C. Liu, J. Xu, Y. Huang, J. Wang and Z. Sun, *Journal of Electronic Materials*, 2012, **41**, 2431.

37. B. Zhang, J. Sun, H. Katz, F. Fang and R. Opila, *ACS applied materials & interfaces*, 2010, **2**, 3170.
38. J. Ouyang, C. W. Chu, F. C. Chen, Q. Xu and Y. Yang, *Advanced Functional Materials*, 2005, **15**, 203.
39. X. Wang and K. Wong, *Thin Solid Films*, 2006, **515**, 1573.
40. J. Ouyang, Q. Xu, C.-W. Chu, Y. Yang, G. Li and J. Shinar, *Polymer*, 2004, **45**, 8443.
41. S. Stankovich, R. D. Piner, X. Chen, N. Wu, S. T. Nguyen and R. S. Ruoff, *Journal of Materials Chemistry*, 2006, **16**, 155.